International Journal of Thermophysics, Vol. 28, No. 2, April 2007 (© 2007)
DOI: 10.1007/s10765-007-0180-4

Use of a High-Temperature Integrating Sphere Reflectometer for Surface-Temperature Measurements

Leonard M. Hanssen,[1,2] Claus P. Cagran,[1] Alexander V. Prokhorov,[1] Sergey N. Mekhontsev,[1] and Vladimir B. Khromchenko[1]

The National Institute of Standards and Technology (NIST) has developed a new facility for the characterization of the infrared spectral emissivity of samples between 150 and 1,000°C. For accurate measurement of the sample surface temperatures above 150°C, the system employs a high-temperature reflectometer to obtain the surface temperature of the sample. This technique is especially useful for samples that have significant temperature gradients due to the thermal conductivity of the sample and the heating mechanism used. The sample temperature is obtained through two measurements: (a) an indirect sample emissivity measurement with an integrating sphere reflectometer and (b) a relative radiance measurement (at the same wavelengths as in (a)) of the sample as compared to a blackbody source. The results are combined with a knowledge of the blackbody temperature and Planck's law to obtain the sample temperature. The reflectometer's integrating sphere is a custom design that accommodates the sample and heater to allow reflectance measurements at temperature. The sphere measures the hemispherical-near-normal (8°) reflectance factor of the sample compared relative to a previously calibrated room-temperature reference sample. The reflectometer technique of sample temperature measurement is evaluated with several samples of varying reflectance. Temperature results are compared with values simultaneously obtained from embedded thermocouples and temperature-drop calculations using a knowledge of the sample's thermal conductivity.

KEY WORDS: emittance; hemispherical-directional reflectance factor; noncontact temperature; Pt-Rh; radiometer; SiC; sphere reflectometer; surface temperature.

[1] Optical Technology Division, National Institute of Standards and Technology, Gaithersburg, Maryland 20899, U.S.A.
[2] To whom correspondence should be addressed. E-mail: hanssen@nist.gov

1. INTRODUCTION

The National Institute of Standards and Technology (NIST) has developed a facility for the characterization of the spectral directional emittance of materials in the infrared for temperatures up to 1,000°C [1,2]. The sample emittance is measured by comparison of the sample spectral radiance to that of a reference blackbody source. If the sample and blackbody are at the same temperature, the emittance is given by the simple ratio of radiances. If there is a difference in temperatures, Planck's function is also used. The uncertainty of the emittance is directly related to the uncertainty in both the sample and blackbody source temperatures. Specifically, the sample surface temperature is not always easily measured with high accuracy. Even with embedded temperature sensors, temperature gradients can be significant between the sensor location and the center of the sample surface, due to a combination of the sample's thermal conductivity, radiant loss, and convective loss. For this reason, we have included a non-contact temperature measurement technique in the facility, which employs an integrating sphere reflectometer. This technique was developed and implemented successfully by Batuello et al. [3,4] at the Istituto di Metrologia "Gustavo Colonnetti" (IMGC), Italy.

In our implementation, we have endeavored to optimize the integrating sphere reflectometer design to obtain the highest possible temperature-measurement accuracy. We have performed Monte Carlo based modeling studies of the sphere, including assessment of response uniformity as a function of baffle design, sphere wall reflectance, and sphere wall specularity [5,6]. The results were used to finalize the sphere design that is being used in the facility. In a companion paper [7], we describe the results of spectral directional emittance measurements of two materials using the facility. In this paper, we describe the sample temperature measurements used in the emittance calculation for the materials. The method is described in Section 2. The instrumentation including the sphere reflectometer is discussed in Section 3. A comparison of the non-contact method, applied to the samples, and contact thermometry is presented in Section 4. An uncertainty evaluation for the temperature method is presented in Section 5. Finally, Section 6 contains our summary and conclusions.

2. MEASUREMENT METHOD

The non-contact measurement method used to obtain the sample temperature involves two steps. First, the sample emittance is measured by means of a sphere reflectometer, and second, the sample radiance is directly

compared with that of a blackbody of known temperature (similar to that of the sample). Both steps utilize a filter radiometer at a (ideally) single wavelength λ to measure the signals from the sample, the reference, and the blackbody. For this paper, all measurements were performed in an air atmosphere but modifications to purge the entire measurement system are underway.

2.1. Sphere Reflectometer—Sample Emittance

A sphere reflectometer is used to compare the hemispherical-directional reflectance factor (see Section 3.1) at near-normal incidence (8°) of the sample at temperature T to that of a calibrated reference standard. Given that the reflectance of the reference standard is known and applying the laws of energy conservation and Kirchhoff, the sample emittance at T can be calculated using the following measurement equation:

$$\varepsilon(\lambda, T) = 1 - \left[\rho_0(\lambda, T_0) \frac{V(\lambda) - V_{\mathrm{ht}}(\lambda)}{V_0(\lambda) - V_{\mathrm{ho}}(\lambda)} \right] \tag{1}$$

where ε is the spectral normal (or 8°) emittance of the sample, λ is the wavelength of the radiometer (and the light source), T and T_0 are the sample and the reference temperatures (T_0 is normally room temperature), ρ_0 is the reflectance of the calibrated reference standard, $V(\lambda)$ and $V_0(\lambda)$ are the signals of the radiometer when viewing the sample and the reference, and $V_{\mathrm{ht}}(\lambda)$ and $V_{\mathrm{ho}}(\lambda)$ are the signal contributions from the empty sample heater and the reference holder, respectively.

2.2. Radiometric Radiance Comparison—Sample Temperature

Utilizing the sample emittance results from the sphere reflectometer, the sample surface temperature can be calculated by a radiometric comparison of the spectral radiance of the sample to that of a blackbody source of known emittance and temperature. Starting off with Planck's radiation law for spectral radiance and accounting for the spectral responsivity of the filter radiometer as well as the blackbody cavity spectral emittance, the measurement equation for this radiometric comparison can be written as

$$\frac{V(\lambda, T)}{V_{\mathrm{BB}}(\lambda, T_{\mathrm{BB}})} = \frac{\varepsilon(\lambda, T)\left(e^{\frac{c_2}{\lambda T_{\mathrm{BB}}}} - 1\right)}{e^{\frac{c_2}{\lambda T_{\mathrm{rad}}}} - 1} \tag{2}$$

where $V(\lambda, T)$ and $V_{BB}(\lambda, T_{BB})$ are the filter radiometer signals for the sample and the blackbody and $\varepsilon(\lambda, T)$ is the sample emittance from the reflectometer measurement. Note: $T \approx T_{rad}$ on the right-hand side's numerator but small heat transfer and convection losses lead to small differences which have to be accounted for in the uncertainty budget.

3. INSTRUMENTATION

3.1. Sphere Reflectometer—Hemispherical-Directional Reflectance Factor and Sample Emittance

The direct emittance measurement is performed through a comparison of the spectral radiance of the sample with that of a reference blackbody source. The sample radiance measurement requires viewing the sample by the detector for a single viewing angle (or field-of-view range). We wished to make use of the same detectors and optical interface for the non-contact temperature measurement as for the radiance measurement. This necessitated the design and use of an integrating sphere for the hemispherical-directional reflectance factor measurement. A schematic of the measurement setup is shown in Fig. 1. The view is partially collapsed. For simplicity, the integrating sphere and blackbody sources, as well as the radiometer stack, are shown in the plane of the paper; the other items all lie in the vertical plane, mounted on an optical breadboard. The integrating sphere and radiometer stack are actually positioned in front of the other optics, while the blackbody source set is positioned behind the optics. This is also shown in Fig. 1 of Ref. [2].

For accurate relative measurements, the sphere reflectometer employs an isotropic sphere design concept which ensures that sample and reference reflected light are equally treated despite possible differences in their scattering distributions (bi-directional reflectance distribution function, BRDF [8,9]). Snail and Hanssen [10] suggest three different designs to accomplish spheres with isotropic throughput. Our design follows their "Design 3," which has $\eta_r = \eta_s \approx 1$ for the reflectometer, where η is the ratio of the reflectance into the detector field-of-view (FOV) to the directional hemispherical reflectance. Snail and Hanssen also describe the equivalent sphere designs (including Design 3) for the hemispherical-directional (h-d) reflectance factor, where the sample and reference are hemispherically illuminated by the source and the measured reflected light is collected in a single direction. In such an h-d configuration, the source and detector are switched compared to a d-h setup. In this case, the hemispherical detector FOV is replaced by a hemispherical illumination from the light source and the two baffles between the light source and the sample and reference

avoid direct illumination of the samples from the source, as illustrated in Fig. 2. In the h-d design, the relative hemispherical-directional reflectance factors $R_{h,d}$ [9] are obtained for the sample and reference, which, according to the reciprocity theorem, equal the directional-hemispherical reflectance [5] and allow us to calculate the sample emittance using Eq. (1) for opaque samples.

During one set of measurements, the directional flux at 8°[3] reflected off of the sample is compared to that of a calibrated reference standard, for which a set of reference samples (with both high and low reflectance, as well as both specular and diffuse) has been calibrated at the Optical Technology Division [11] of the National Institute of Standards and Technology (NIST) in the 0.6 to 2.5 μm range. For all measurements reported herein, a specular gold mirror was used as the reference sample. Since no polarizers were used for the reported measurements, the mean of s and p reflectance values was used as a reference value. A gold-coated flip mirror in the interface optics is used to switch between the sample, the reference, and the blackbody. Either a radiometer with a Si-detector (including a narrow band-pass filter) at 905 nm or an InGaAs-radiometer at 1,550 nm is used depending on the actual temperature of the sample.

Since the goal is to measure the sample temperature, it does not matter what wavelength this is done at, except to the extent it affects the temperature measurement itself: (a) the shorter the wavelength, the smaller

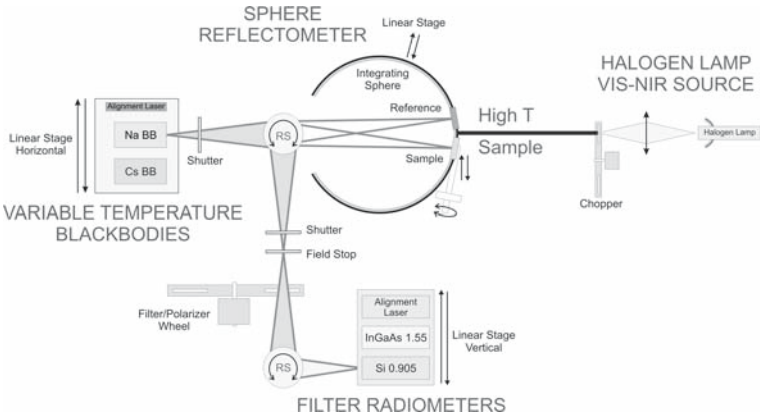

Fig. 1. Schematic of the sphere reflectometer and the setup used for the radiometric temperature measurement of a heated sample; RS: rotation stage with mirror.

[3] This angle is sufficient to guarantee that, as viewed from the detector, a specular sample is fully illuminated with light from the sphere and not shaded by the exit port.

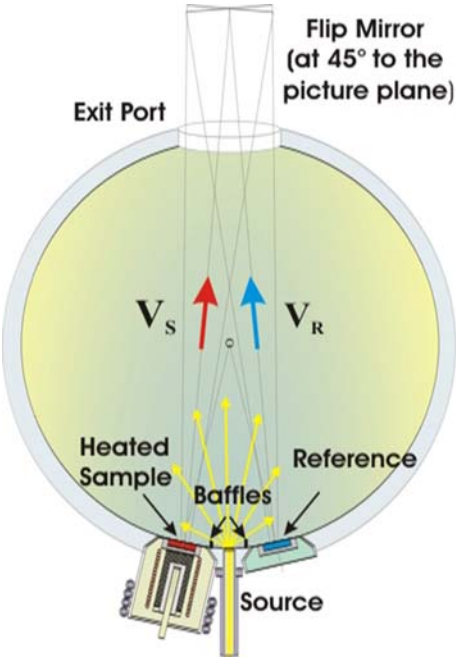

Fig. 2. Cross-sectional view of the sphere reflectometer showing details of the sample heater, reference holder, fiber source, and baffles in position. Measurements consist of sample-to-reference signal ratios obtained via tilting of the exit flip mirror.

the temperature uncertainty for a given reflectance uncertainty; (b) both reflectance and radiance need to be measured at the same wavelength, i.e. both non-zero. Since material properties vary spectrally, having several wavelengths at hand allows greater flexibility in accommodating the sample characteristics. The two radiometers at 905 and 1,550 nm, as well as a small monochromator (especially useful for item (b)), are available to meet these requirements, but only the radiometers were used for the herein reported measurements.

A halogen lamp with a gold reflector (to enhance the infrared (IR) component of the reflected light) is coupled to a diffuser located at the sphere wall between the two samples by means of a fiber bundle which is used as the light source. After a warm-up time of about 30 min, this source is very stable and reproducible within a few hundredths of a percent.

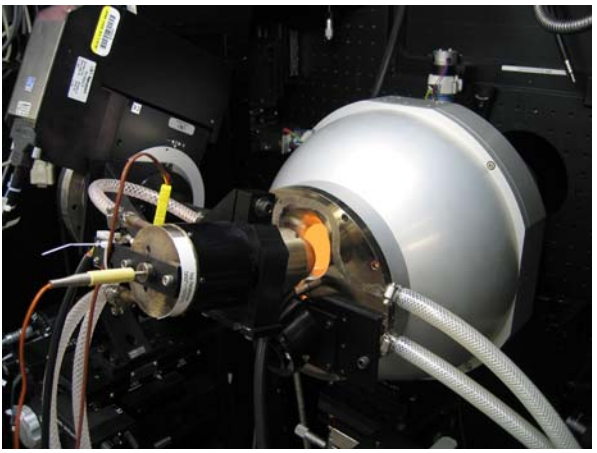

Fig. 3. Photo showing the rear section of the sphere reflectometer with the sample heater removed a short distance from its measurement position. The darker water-cooled flange contains the sample, reference, and source input ports. To the left, the sample rotation stage for variation of the viewing angle for the spectral emittance measurements can be seen.

Effects related to from the two holders for the sample and reference proved to be more significant, since they contribute a small portion to the overall signal and are not identical. Estimates for the contributions of the holders were obtained by removing the sample and letting the detector view the empty holder (the holders are hollow and the view is projected onto a black surface behind the sphere). The out-of-optical-field scattered signal thus obtained was recorded for both holders and later subtracted from the reflectance factor signals as in Eq. (1).

3.2. Instrumental Setup for Non-contact Temperature Measurement

After the sample emittance has been measured with the sphere reflectometer which is pictured in Fig. 3, the sphere is moved out of the optical beam path by means of a linear stage, while the sample heater maintains its position and angle[4] with respect to the flip mirror. The same setup as shown in Fig. 1 is then used to compare the radiance from the sample to the radiance of a blackbody by means of the radiometers. The only difference in the setup is the introduction of a low-reflectance baffle between

[4] In most cases sample emittances are angle-dependent and exactly the same geometry as in the reflectance measurement must be used to avoid introducing a systematic error.

Table I. Results from the Sphere Reflectometer Characterization at Room Temperature

Wavelength (nm)	Mirrors Ratio	Diff. (%)	Specular/ Diffuse	Calibration Data	Diff. (%)	SiC vs. Gold	Calibration Data	Diff. (%)
905	1.0004	0.04	1.0102	1.0100	0.02	0.1929	0.1930	−0.05
1550	1.0007	0.07	1.0165	1.0220	−0.55	0.1934	0.1937	−0.16

the sample and the flip mirror to minimize the scattered light contribution to the radiometer background signal from the sample emitted radiation as well as to reduce inter-reflections between the sample and other system hardware.

4. RESULTS

4.1. Reflectometer Characterization

Before using the reflectometer at elevated temperatures, we characterized its performance at room temperature first with calibrated samples in both ports (reference and actual sample ports). This characterization included positioning and alignment of the sample in its dedicated holder as well as positioning, angle, and alignment of the holder in the sphere port. All of the above mentioned parameters are found to affect the reflectance result but can be minimized through careful adjustment and alignment of the sphere prior to measurements.

To test the alignment accuracy and holder corrections and evaluate the reflectometer accuracy, we performed several measurements with results as shown in Table I. Two radiometers (Si at 905 nm and InGaAs at 1,550 nm) were used for this study. Two nominally identical Al mirrors from the same batch were compared and their signals ratioed, expecting a number close to one. We examined the case of a specular sample (unprotected gold mirror) versus a diffuse reference (sintered PTFE). In this specific case, additional optical sphere design parameters such as the exit port size, the baffles between the ports and the light source, and especially the reflectance of the sphere coating come into play. Earlier modeling data of the sphere [6] and its design show that a deviation of about 1% can be expected for the extreme diffuse/specular case depending on the actual reflectance of the sphere coating. The 1% correction is included in Table I. Finally, a SiC sample at room temperature was measured versus a calibrated gold reference standard; the SiC sample was calibrated with a second sphere setup used for absolute spectral reflectance [5, 12].

The reflectance factor measurement becomes more complicated when using a heated sample, since the heater itself has a different geometry from the room-temperature reference sample holder and the screws holding the sample penetrate into the sphere, thus slightly disturbing the overall sphere geometry and throughput. Two sets of measurements at room temperature were performed to estimate the signal contribution arising from the heater: (i) the sample and the reference in their room-temperature holders, and (ii) the sample mounted in the heater and the reference in its holder. In both cases, the measured reflectance ratio of the sample to reference was calculated and the difference in the result was later used as the contribution from the heater in Eq. (1). This approach appears to correct most of the potential error due to out-of-field scatter; however, it does not account for temperature-dependent changes in the heater contribution.

4.2. SiC and Pt-10%Rh

The sample materials under investigation were a disc-shaped (19 mm diameter, 2.3 mm thick disc) sample of β-SiC manufactured by General Electric Co. [13] around 1984 from submicrometer β-SiC power with small additions ($\sim$0.5 wt% each) of boron and carbon, which was sintered in a reducing atmosphere at approximately 2,100°C [14], provided by NIST's Ceramics Division [15] and a disc-shaped (2.3 mm thickness, 19 mm diameter) Pt-10%Rh ZGS sample purchased from Noble Metals NA, West Chester, Pennsylvania [13]. The actual measured surface of the samples is polished. In addition to the sphere reflectometer measurement and the radiometric temperature determination, the sample temperatures have also been monitored by means of Type K thermocouples (TC) within a cavity-hole (0.7 mm diameter, 8 mm depth) machined into the side of each sample.

The measurement procedure for each sample at each individual temperature consists of using the sphere reflectometer to first measure the sample reflectance and calculating its emittance (see Eq. (1)) and using this result later in the radiometric comparison to calculate the sample surface temperature. The results of the reflectometer measurements are shown in Fig. 4. The SiC emittance is nearly constant versus temperature and wavelength as compared to the Pt-10Rh dependences.

Although the samples are only 2.3 mm in thickness, a temperature difference between the temperature reading of the TC and the radiometric surface temperature measurement can be expected due to the effects of heat conduction and convection from the sample surface. This difference can theoretically be estimated by using heat transfer models and equations.

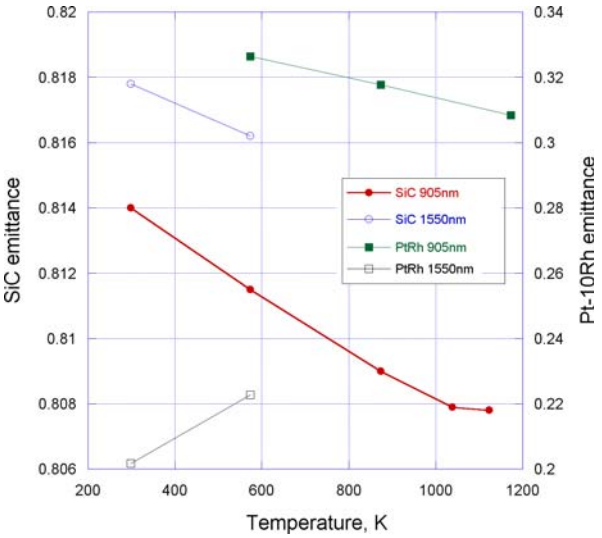

Fig. 4. Sample emittance for SiC and Pt-10Rh at various temperatures measured with the sphere reflectometer. These results are used to calculate the surface temperature T_{radio} in the radiometric comparison with a variable temperature blackbody.

Basic estimations have been made using an equation from Ref. [16]:

$$(T_{\text{TC}} - T_{\text{surf}})\,\frac{k}{x} = \varepsilon\sigma\left(T_{\text{surf}}^4 - T_{\text{amb}}^4\right) \tag{3}$$

where T_{TC} is the thermocouple temperature, T_{surf} is the desired surface temperature of the sample, k is the thermal conductivity, x is the distance between the thermocouple position and the surface, ε is the sample emittance, σ is the Stefan-Boltzmann constant, and T_{amb} is the ambient temperature.

This basic equation can be modified by also adding convection contributions from a flat surface and by solving the boundary problem by means of iteration. A simple computer program that also utilizes the convective heat transfer coefficient, h, as an input value was used to calculate the surface temperature. The input parameters used for these calculations are shown in Table II.

Although emittance (near-normal emittance at 8°) values at the respective temperatures have been obtained with the sphere reflectometer, these values cannot be used for the temperature-drop calculations, since total emittance values are needed in Eq. (3). Instead, total emissivities from Refs. [18] and [19] have been used exclusively for the SiC and

Table II. Input Parameters for Surface Temperature Calculations for SiC and Pt-10%Rh

	SiC	Pt-10%Rh[a]
k ($W \cdot m^{-1} \cdot K^{-1}$)	134	72
h ($W \cdot m^{-2} \cdot K^{-1}$)[b]	17	17
x (mm)	1.15	1.15
T_{amb} (K)	293	293

[a]Since no data for the actual Pt-10%Rh alloy were available, k for pure Pt [17] was used instead.
[b]Convective heat-transfer-coefficient data were estimated for air at the ambient atmosphere using formulas and tabulated data from Ref. [16]. Note: h itself is temperature-dependent, and for simplicity, only the value at the highest temperature is given.
k: thermal conductivity, h: convective heat transfer coefficient, x: distance between TC and sample surface, and T_{amb}: ambient temperature.

Table III. Summary of Temperature Results from Model Calculations, TC Readings, and Radiometer Measurements

Material	T_{TC} (K)	ε_{tot}	$T_{w/oconv.}$ (K)	$T_{w/conv.}$ (K)	T_{radio} (K)	$\Delta T_{(radio-conv)}$ (K)
SiC	298.00	0.800	298.00	298.00	–	–
	573.75	0.800	573.71	573.67	573.38	−0.29
	868.56	0.800	868.34	868.26	867.94	−0.32
	1038.81	0.800	1038.36	1038.25	1038.04	−0.21
	1123.61	0.800	1122.99	1122.87	1122.07	−0.80
Pt-10%Rh	573.59	0.096	573.58	573.51	572.96	−0.54
	872.76	0.129	872.69	872.54	871.83	−0.71
	1172.75	0.172	1172.45	1172.21	1171.75	−0.47

T_{TC}: temperature from thermocouple in sample, ε_{tot}: total emittances from literature data, for SiC [18] and for Pt-10Rh [19], $T_{w/o\,conv.}$: temperature calculation due to thermal gradient without convective losses, $T_{w/conv.}$: temperature calculation due to thermal gradient including convective losses, T_{radio}: temperature measurement with radiometer, and $\Delta T_{(radio-conv)}$: temperature difference between radiometer measurement and calculation including convection.

Pt-10%Rh samples. The measured and calculated temperature results are collectively listed in Table III.

5. UNCERTAINTY ANALYSIS

5.1. Sample Temperature with Thermocouples

The thermocouples are commercially available units from Omega (KMQIN-020U-6) [13] with special limits of uncertainty (according to ASTM International, E-230), the greater of 1.1°C or 0.4%.

5.2. Model-Based Sample Surface Temperatures

Since the exact uncertainty for the model-based calculations is difficult to evaluate (there are no analytical solutions to the derivative of the formula) a minimum/maximum calculation was performed to estimate the uncertainty. The following uncertainties are used for the input parameters: total emittance 10%, thermal conductivity 20%, convective heat transfer coefficient 20%, and thermocouple position 10%. Finally, the uncertainty of the thermocouple temperature is given by the manufacturer as the greater of 1.1°C or 0.4%, which cannot be used directly for this uncertainty budget because there are two overlaying effects. First, a change in the thermocouple reading mainly offsets the result and second, the temperature difference between the thermocouple and the surface temperature shifts slightly. The latter is what should be considered for our uncertainty budget.

The listed uncertainties have been used to calculate the variation in the surface temperature at two different thermocouple temperatures (close to 573.15 K and at the maximum temperature). The combined uncertainty ($k = 2$) for all these components is 236 mK at 573.752 K and 869 mK at 1123.605 K for the SiC sample, and 212 mK at 573.590 K and 788 mK at 1172.747 K for the Pt-10%Rh sample.

5.3. Sample-Temperature Measurement with Radiometer and Sphere Reflectometer

The uncertainty budget for the sample-temperature measurement with the radiometer is lengthy and explained in full in Ref. [7], of which only a short summary is presented within this section. The uncertainty consists primarily of four different components, from the repeatability of the temperature measurement, the reflectance measurement, the radiometer calibration, and the size-of-source-effect (scatter) of the interface optics; and each of these four components may have different contributions. The actual numbers for the different components, the combined standard uncertainty for the spectral emittance measurement and the expanded uncertainties for Pt-10%Rh and SiC at 600°C are listed in Table IV.

These uncertainties in emittances at a given wavelength convert to uncertainties in temperature by using the following equation:

$$\frac{\mathrm{d}\varepsilon(\lambda)}{\varepsilon(\lambda)} = \frac{c_2}{\lambda}\frac{\mathrm{d}T(\lambda)}{T(\lambda)^2} \tag{4}$$

where $\mathrm{d}\varepsilon(\lambda)/\varepsilon(\lambda)$ is the relative uncertainty of emittance at the wavelength λ, c_2 is Planck's second radiation constant ($c_2 = 1.4387752 \times 10^{-2}$ m·K

Table IV. Uncertainty Budget of the Sample Spectral Directional Emittance Measurement including the Sphere Reflectometer

Uncertainty budget of sample spectral emittance Reflectometer at 905 nm	Type	Pt-10%Rh at 600°C	SiC at 600°C
Repeatability of temperature comparison	A	0.05%	0.05%
Sample reflectance			
Repeatability of reflectance comparison	A	0.03%	0.03%
Sample			
Alignment	B	0.19%	0.19%
Temperature	B	0.05%	0.00%
Reflectance reference			
Calibration	B	0.09%	0.09%
Alignment	B	0.19%	0.19%
Sphere reflectometer	B	0.20%	0.20%
Radiometer calibration			
Calibration at FP	B	0.01%	0.01%
Interpolation	B	0.01%	0.01%
Alignment	B	0.00%	0.00%
SSE of interface optics	B	0.04%	0.04%
Combined standard uncertainty of spectral emittance		0.36%	0.35%
Expanded uncertainty ($k = 2$)		0.72%	0.70%

All reported uncertainties are signal-related (relative) and based on a sample temperature of 600°C and the Si-radiometer (905 nm). Uncertainties for the InGaAs radiometer are only marginally different and therefore not explicitly reported.

Table V. Expanded ($k = 2$) Absolute Uncertainties ΔT in Radiometric Temperatures T for SiC and Pt-10Rh

SiC T (K)	ΔT (K)	Pt-10Rh T (K)	ΔT (K)
573.75	0.14	573.59	0.15
868.56	0.34	872.76	0.34
1038.81	0.49	1172.75	0.61
1123.61	0.57		

[20]), T(λ) is the temperature at the wavelength λ, and $\mathrm{d}T(\lambda)$ is its uncertainty (absolute). This approach disregards the ratio $\exp(c_2/\lambda T)/\{\exp(c_2/\lambda T) - 1\}$ in Eq. (4), as its maximum contribution at 1172.747 K is only 1.3×10^{-6}%. The total expanded uncertainties for the radiometric temperature measurements are listen in Table V.

6. SUMMARY AND DISCUSSION

A recently implemented hemispherical-directional sphere reflectometer has been thoroughly characterized and used to indirectly measure the near-normal, spectral emittance of a sample by comparison to a calibrated reference standard. Although these emittance results are also of interest, they are used in a second step of a method to accurately measure surface temperatures by means of a radiance comparison with a blackbody using a filter radiometer.

Previously, all of our sample-temperature measurements relied on contact thermometry from placement of a thermocouple in a small cavity-like hole in the side of each sample. It is known that reliance on these embedded temperature sensors can lead to significant temperature errors. Temperature gradients between the sensor location and the center of the sample surface can occur from a combination of the sample's thermal conductivity, radiant loss, and convective loss.

Both contact and non-contact methods for sample temperature measurements have been experimentally investigated within this work, permitting a direct comparison of the two methods for the first time at NIST. Additionally, the theoretically expected surface temperatures have been calculated based on a modified heat-transfer equation including radiative and convective heat losses from the surface and the thermocouple readings.

As a result of this comparison, it can be seen that the surface temperatures detected by the radiometer are always lower than the thermocouple readings and the difference increases as the temperature rises, a behavior that can be anticipated. Although the absolute differences between the non-contact temperature and radiometer are not large for SiC and Pt-Rh, the situation can be worse for other materials. When comparing the radiometer results with the model-based calculated surface temperatures, the temperature differences become smaller and the results are in good agreement within the estimated uncertainties for all the methods.

Finally, the comprehensive uncertainty analysis also clearly indicates the advantage of the radiometric method over the thermocouple and the model-based calculation, since the uncertainties for the radiometer temperatures are always smaller than the minimum TC uncertainty of 1.1°C for the Type K TC that was used. This uncertainty can be improved by using Type S TCs instead, whose minimum uncertainty is 0.6°C[5] but which are more difficult to handle since their electric signal output is considerably less than for the Type K TCs. The uncertainties for the model-based temperatures are comparable to the radiometer uncertainties, but strongly depend on the accuracy and availability of input data for each

[5] The greater of 0.6°C or 0.1% in the range from 0 to 1,450°C.

material. Specifically for materials with poor thermal conductivity, contact thermometry will have even larger uncertainties.

REFERENCES

1. L. M. Hanssen, S. G. Kaplan, and S. N. Mekhontsev, In B. Fellmuth, J. Seidel, and G. Scholz, eds. *Proc. 8th Int. Symp. Temp. Thermal Meas. Ind. Sci.* (*TEMPMEKO 2001*), Berlin, (2001), pp. 265–270.
2. L. M. Hanssen, S. N. Mekhontsev, and V. B. Khromchenko, *Proc. SPIE* **5405**:1 (2004).
3. M. Batuello, F. Lanza, and T. Ricolfi, In *Proc. 2nd Int. Symp. Temp. Thermal Meas. Ind. Sci.* (*IMEKO TC12*), Suhl, Germany, (1984), pp. 125–130.
4. M. Batuello and T. Ricolfi, *High Temp.—High Press.* **21**:303 (1989).
5. A. V. Prokhorov, S. N. Mekhontsev, and L. M. Hanssen, In B. Fellmuth, J. Seidel, and G. Scholz, eds. *Proc. 8th Int. Symp. Temp. Thermal Meas. Ind. Sci.* (*TEMPMEKO 2001*), Berlin, (2001), pp. 277–282.
6. A. V. Prokhorov, S. N. Mekhontsev, and L. M. Hanssen, *Appl. Optics* **40**:3832 (2003).
7. C. P. Cagran, L. M. Hanssen, M. Noorma, A. V. Gura, and S. N. Mekhontsev, *Int. J. Thermophys.* **28**:2 (2007) doi:10.1007/s10765-007-0183-1
8. CIE, *International Lighting Vocabulary* (CIE Publication No. 17.4, Geneva, 1987).
9. L. M. Hanssen and K. A. Snail, in Handbook of Vibrational Spectroscopy, Vol. 2, J. M. Chalmers and P. R. Griffiths, eds. (John Wiley & Sons, Ltd., Chichester, United Kingdom, 2002), pp. 1175–1192.
10. K. A. Snail and L. M. Hanssen, *Appl. Optics* **28**:1793 (1989).
11. M. E. Nadal, Optical Technology Division, National Institute of Standards and Technology, Gaithersburg, MD: http://physics.nist.gov/Divisions/Div844/facilities/specphoto/specphoto.html
12. L. Hanssen, A. Prokhorov, V. Khromchenko, and S. Mekhontsev, In D. Zvizdic, ed. *Proc. 9th Int. Symp. Temp. Thermal Meas. Ind. Sci.* (*TEMPMEKO 2004*),Dubrovnik, Croatia, (2004), pp. 539–544.
13. Certain commercial equipment, instruments, or materials are identified in this paper to specify the experimental procedure adequately. Such identification is not intended to imply recommendation or endorsement by the National Institute of Standards and Technology, nor is it intended to imply that the materials or equipment identified are necessarily the best available for the purpose.
14. M. J. Slavin and G. D. Quinn, *Int. J. High Technol. Ceram.* **2**:47 (1986).
15. Ceramics Division (852), National Institute of Standards and Technology, Gaithersburg, MD: http://www.ceramics.nist.gov/
16. F. P. Incropera and D. P. DeWitt, *Fundamentals of Heat and Mass Transfer, 4th Ed.* (John Wiley & Sons, New York, 1996).
17. The Platinum Metals Group (PGM) Online Database: http://www.platinummetalsreview.com/jmpgm/index.jsp
18. Y. S. Touloukian and D.P. DeWitt, eds. *Thermophysical Properties of Matter*, Vol. 8, *Thermal Radiative Properties—Nonmetallic Solids* (IFI/Plenum, New York-Washington, 1972).
19. Y. S. Touloukian and D. P. DeWitt, eds. *Thermophysical Properties of Matter*, Vol. 7, *Thermal Radiative Properties—Metallic Elements and Solids* (IFI/Plenum, New York-Washington, 1970).
20. CODATA International Recommended Values of the Fundamental Physical Constants, Online Database: http://physics.nist.gov/cuu/Constants/